Electrostatically Actuated Resonant Microcantilever Beam in CMOS Technology for the Detection of Chemical Weapons

Ioana Voiculescu, Mona E. Zaghloul, *Fellow, IEEE*, R. Andrew McGill, Eric J. Houser, and Gary K. Fedder

Abstract—The design, fabrication, and testing of a resonant cantilever beam in complementary metal–oxide semiconductor (CMOS) technology is presented in this paper. The resonant cantilever beam is a gas-sensing device capable of monitoring hazardous vapors and gases at trace concentrations. The new design of the cantilever beam described here includes interdigitated fingers for electrostatic actuation and a piezoresistive Wheatstone bridge design to read out the deflection signal. The reference resistors of the Wheatstone bridge are fabricated on auxiliary beams that are immediately adjacent to the actuated device. The whole device is fabricated using a 0.6-μm, three-metal, double-poly CMOS process, combined with subsequent micromachining steps. A custom polymer layer is applied to the surface of the microcantilever beam to enhance its sorptivity to a chemical nerve agent. Exposing the sensor with the nerve agent simulant dimethylmethylphosphonate (DMMP), provided a demonstrated detection at a concentration of 20 ppb or 0.1 mg/m^3. These initial promising results were attained with a relatively simple design, fabricated in standard CMOS, which could offer an inexpensive option for mass production of a miniature chemical detector, which contains on chip electronics integrated to the cantilever beam.

Index Terms—Cantilever beam, complementary metal–oxide semiconductor (CMOS) technology, electrostatic actuation, gas sensor, nerve agent.

I. INTRODUCTION

IN order to allow widespread monitoring capacity, an inexpensive and small sensing approach to detection is needed. Using a micromachined sensor or system is a possible solution to this need and provided the motivation for this work.

There is an acute need for highly sensitive, accurate, and rapid detection techniques for chemical agents, toxic industrial chemicals, and explosives. The onset of clinical responses after exposure to hazardous chemicals is often rapid, so it is desirable to have a large number of detectors covering wide geographical areas, or for the individual to wear the detector as an unobtrusive pager like device. For cost and size issues, it is attractive to consider the use of micromachined technologies which offer the capability for on chip electronics to lower costs and provide high production yields.

A chemical sensor is a device, which converts chemical information into an analytically useful signal [1]. Chemical sensors are important for a variety of industrial and environmental applications, including the detection of hazardous chemicals, quality control in the food, perfume, and beverage industries, and medical applications [2].

A typical configuration for a chemical sensor includes a sorbent layer deposited on an active area of a transducer [3]. The interaction of a gas and the sorptive layer is monitored as a function of a physical change in the coating, and transduced into an electrical signal for ease of recording or display. For active gas sampling, pneumatic connections and a gas pump are normally required to make air flow over the chemical sensor. Conventional chemical sensors utilize transducers which are relatively large and have millimeter sized dimensions [4]. The advent and maturation of microelectromechanical systems (MEMS) technology now offers many opportunities to dramatically reduce the size, cost, and power consumption of chemical sensors [5]–[10]. Current state-of-the-art chemical detectors are typically hand held systems.

II. SENSOR TECHNOLOGY AND DESCRIPTION

A. Principles of the Microcantilever Beam Gas Sensor

A cantilever beam chemical sensor consists of two key components: a gas sorptive layer, such as a polymer, and the cantilever beam transducer. Two modes of operation of the cantilever beam can be distinguished [10]. In the static mode, the bending of the cantilever beam upon mass loading and related surface stress is measured. In the dynamic mode, the cantilever beam can be actuated at its fundamental resonant frequency. The fundamental resonant frequency in turn depends on the mass loading of the cantilever beam.

The beam structures fabricated in this work were designed with a range dimensions to explore the effect of device shape on resonant frequency, and mass sensitivity. Six different designs were included in a single chip. Short, wide, and thick cantilever beams are preferred for higher resonant frequencies, and large surface structures which maximize the area for polymer coating and subsequent gas sorption. In this regard, the length (L) and

I. Voiculescu is with the Department of Mechanical and Aerospace Engineering, The George Washington University, Washington, DC 20052 USA (e-mail: ioana@gwu.edu).

M. E. Zaghloul is with the Department of Electrical and Computer Engineering, The George Washington University, Washington, DC 20052 USA (e-mail: zaghloul@gwu.edu).

R. A. McGill and E. J. Houser are with the Naval Research Laboratory, Washington, DC 20375 USA (e-mail: mcgill@nrl.navy.mil; ejhouser@nrl.navy.mil).

G. K. Fedder is with the Department of Electrical and Computer Engineering, Carnegie Mellon University, Pittsburgh, PA 15213-3890 USA (e-mail: fedder@ece.cmu.edu).

Report Documentation Page		*Form Approved* *OMB No. 0704-0188*

Public reporting burden for the collection of information is estimated to average 1 hour per response, including the time for reviewing instructions, searching existing data sources, gathering and maintaining the data needed, and completing and reviewing the collection of information. Send comments regarding this burden estimate or any other aspect of this collection of information, including suggestions for reducing this burden, to Washington Headquarters Services, Directorate for Information Operations and Reports, 1215 Jefferson Davis Highway, Suite 1204, Arlington VA 22202-4302. Respondents should be aware that notwithstanding any other provision of law, no person shall be subject to a penalty for failing to comply with a collection of information if it does not display a currently valid OMB control number.

1. REPORT DATE **07 NOV 2004**	2. REPORT TYPE	3. DATES COVERED **00-00-2004 to 00-00-2004**
4. TITLE AND SUBTITLE **Electrostatically Actuated Resonant Microcantilever Beam in CMOS Technology for the Detection of Chemical Weapons**		5a. CONTRACT NUMBER
		5b. GRANT NUMBER
		5c. PROGRAM ELEMENT NUMBER
6. AUTHOR(S)		5d. PROJECT NUMBER
		5e. TASK NUMBER
		5f. WORK UNIT NUMBER
7. PERFORMING ORGANIZATION NAME(S) AND ADDRESS(ES) **Carnegie Mellon University,Department of Electrical and Computer Engineering,Pittsburgh,PA,15213-3890**		8. PERFORMING ORGANIZATION REPORT NUMBER
9. SPONSORING/MONITORING AGENCY NAME(S) AND ADDRESS(ES)		10. SPONSOR/MONITOR'S ACRONYM(S)
		11. SPONSOR/MONITOR'S REPORT NUMBER(S)
12. DISTRIBUTION/AVAILABILITY STATEMENT **Approved for public release; distribution unlimited**		
13. SUPPLEMENTARY NOTES		
14. ABSTRACT **see report**		
15. SUBJECT TERMS		

16. SECURITY CLASSIFICATION OF:			17. LIMITATION OF ABSTRACT	18. NUMBER OF PAGES	19a. NAME OF RESPONSIBLE PERSON
a. REPORT **unclassified**	b. ABSTRACT **unclassified**	c. THIS PAGE **unclassified**	**Same as Report (SAR)**	**7**	

Standard Form 298 (Rev. 8-98)
Prescribed by ANSI Std Z39-18

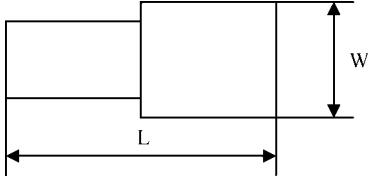Fig. 1.   Basic beam dimensions L and W.

the width (W) of the cantilever beam are varied in order to determine the optimal dimensions for these structures; see Fig. 1. L is varied between 130 and 300 μm, and W is varied from 60 to 150 μm.

A thin layer of sorptive polymer is coated on the beam plate surface. This results in a frequency shift of the device to a new signal baseline. In the absence of actual polymer thickness measurements, it is typical to quote the amount of polymer coated as a frequency shift. The uptake of different gases is monitored as an additional shift in the device frequency, which is reversible if the gas-polymer chemical interactions are reversible. The cantilever beam gas sensor acts as a resonating microbalance, with mass increases normally leading to a decrease in the cantilever beam resonant frequency.

The amount of gas mass sorbed to the cantilever beam can be determined from the frequency shift of the cantilever beam, and if a calibration curve has been developed, the concentration of the gas in the air can be computed.

The natural frequency of a simple undamped rectangular cantilever beam is defined as [11]

$$f = \frac{3.51}{2\pi} \sqrt{\frac{EI}{mL^4}} \qquad (1)$$

where E, I, m, and L are the Young's modulus, the moment of inertia about the neutral axis, the mass per unit length, and the length of the cantilever beam, respectively.

The natural frequency for the free undamped vibration of a composite cantilever beam can be expressed by replacing the bending stiffness (EI) and mass per unit length (m) terms from (1) with composite bending stiffness and composite mass per unit length. The resonant frequency for a composite cantilever beam is given by (2)

$$f = \frac{3.51}{2\pi} \sqrt{\frac{\sum\limits_{i=1}^{N} E_i I_i}{L^4 \sum\limits_{i=1}^{N} m_i}} \qquad (2)$$

where N is the number of layers of the composite cantilever beam, E_i, I_i, and m_i are the effective Young's modulus, the moment of inertia and the mass per unit length, of each layer, respectively [12]–[15].

For a microcantilever beam, and a uniformly deposited mass, the gravimetric change Δm can be estimated with (3) [16]

$$\Delta m \approx \frac{k}{\pi^2} \left(\frac{1}{f_1^2} - \frac{1}{f_2^2} \right) \qquad (3)$$

where f_1 and f_2 are the resonant frequencies of the cantilever beam after and before absorption and k is the spring constant.
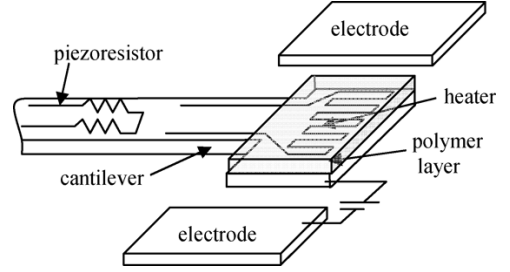

Fig. 2.   Cantilever beam gas sensor. Electrodes are used for electrostatic actuation of the beam.

The spring constant k for a composite cantilever beam with a uniform cross section is given by [13]

$$k = \frac{3 \sum\limits_{i} E_i I_i}{L^3} \qquad (4)$$

E_i and I_i denoting the effective Young's modulus and the moment of inertia of the individual layers of the beam, respectively. The amount of gas sorbed in the polymer depends on the specific gas-polymer interaction(s), the amount of polymer, and the gas concentration in the environment [3]. At a molecular level, the gas diffuses in and out of the polymer film, and the concentration in the polymer rises until a dynamic equilibrium is reached. For gases that are strongly bound to the polymer, desorption can be facilitated by the operation of a heater. In a cantilever beam's. array format with each beam coated with a different polymer, the pattern of responses or fingerprint that results from a gas exposure can be used to identify the gas.

A diagram of the cantilever beam, which is employed in this work, is shown in Fig. 2. Electrostatic actuation is used to drive the cantilever beam in a resonant mode. The resonant frequency is measured by a set of piezoresistors connected in a Wheatstone bridge configuration. Only the beam tip is coated with the thin layer of sorbent polymer.

B. Design and Fabrication of Complementary Metal–Oxide Semiconductor (CMOS) Cantilever Beam Gas Sensor Chip

CMOS technology is the most common fabrication technology for integrated circuits. Its combination with post-process micromachining allows for integration of sensors and circuitry on the same chip. Micro structures integrated with CMOS are commonly made from multilayers of silicon oxide, silicon nitride, polysilicon, and aluminum thin films.

The chip was designed in the Carnegie Mellon University (CMU) CMOS-MEMS technology using MEMSCAP-Xplorer software installed under Cadence. Typical die size for this process is 2.5×2.5 mm. The foundry used in this work is based on the Austrian Microsystems (AMS) process (0.6 μm, three-metal, double-poly CMOS). The standard CMOS-MEMS process is followed by two maskless dry etch steps to release the microstructures that are protected by the top-most metal layer. The RIE postprocessing steps were performed at CMU [17]. In the chip layout, suitable gaps are included to permit the RIE post processing steps. An anisotropic reactive ion etch (RIE) with CHF_3 and O_2 is first used to remove the silicon oxide not covered by any of the aluminum metal layers. This step is followed by an isotropic RIE process using SF_6 and O_2 to remove the underlying silicon, and release the microstructure.
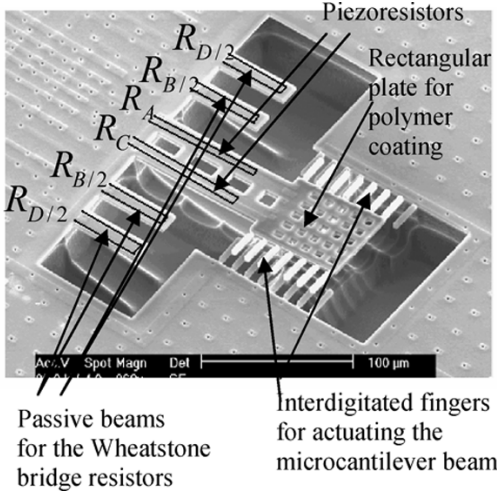
Fig. 3. SEM image of beam 6. The resistors, which are part of the Wheatstone bridge, are marked to correspond to Fig. 4.

The key to the CMU CMOS-MEMS process is in the use of metallization as an etch-resistant mask to define the microstructures. The CMU CMOS-MEMS process has been described previously in detail [18].

The microstructural layers can be designed with any of the three metal layers as the etch mask, with their thickness being a function of the number of metal masking layers. In most surface micro-machined technologies, the design control is limited to two planar dimensions of a mechanical structure. An advantage of the CMU CMOS technology is based on the availability of up to three metal layers, which offers the design flexibility in a third dimension. Using different combinations of the three metal layers, different beam thicknesses can be fabricated. In this work, the metal layer combinations of M1 and M3 were used to generate devices with a thickness of 4.2 μm [19].

The post-processed structures fabricated using CMU CMOS-MEMS technology with the AMS CMOS process have the drawback that they typically exhibit bending after release. The CMOS metal and dielectric layers, which form the laminated structures, have different coefficients of thermal expansion, which result in the bending of the released structures [20]. However, the cantilever beam is electrostatically actuated perpendicular to the bending of the beam structures, so the device bending is not a negative design issue for this application.

Six different designs of chemical sensors were included in a single test chip. An example cantilever beam, number 6, is shown in Fig. 3.

The cantilever beam is driven electrostatically, using the two sets of interdigitated fingers seen in Fig. 3. The fingers designed on the chip substrate, which are flat, are wired to the ground pad. The fingers, designed on opposite sides of the cantilever beam are tilted out of the device plane and are wired together to a single bond pad, which is connected to an ac drive voltage superimposed on a dc voltage.

C. Design and Implementation of On-Chip Wheatstone Bridge

The resonant frequency is monitored with a highly symmetrical on-chip Wheatstone bridge arrangement. Each device on the fabricated chip includes a Wheatstone bridge arrangement.
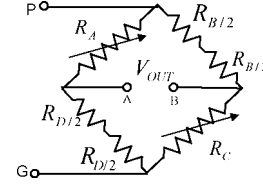

Fig. 4. On-chip Wheatstone bridge arrangement (compare with Fig. 3).

The Wheatstone bridge transduces any change in resistance due to the strain experienced by the piezoresistors, which can be manifested by deflection or oscillation [21]. Using the Wheatstone bridge configuration, the relative change in the resistance of the piezoresistor is provided as an output voltage signal. Figs. 3 and 4 show the circuit and associated components of the device.

The full Wheatstone bridge has two piezoresistors R_A and R_C positioned on the active cantilever beam, and two reference resistors R_B and R_D which are situated on neighboring short, auxiliary beams, as shown in Fig. 3.

Two resistors connected in series are provided for each reference resistor and positioned in the common-centroid arrangement to allow for improved resistance matching.

This particular Wheatstone bridge design used in this work positions all of the resistors on beams, so that on release, each resistor experiences the same changes in stress, and results in a similar degree of bending; see Fig. 3. This design allows the resistors to maintain their matched values before and after release. For the electrical characterization of the cantilever beam gas sensors, the applied voltage at the input of the Wheatstone bridge was set at 6 V. The offset voltage of the Wheatstone bridge, when the cantilever beam was not actuated was between 2 – 20 mV, depending on the cantilever beam design.

The resistance measurements were performed with a Summit 11 651–6 Thermal Probe Station, with a Keithley 2400 source meter, using Cascade Microtech DCP 150R Precision DC probes.

III. SIMULATION AND MEASUREMENT OF THE CANTILEVER BEAM RESONANT FREQUENCIES

A. Finite-Element Simulation of the Cantilever Beams Resonant Frequencies

It is important to identify the true resonant mode of the cantilever beams for any experimental measurements. The resolution of the experimental measurements will be poor if the resonant frequencies are not known. Without this knowledge, a large bandwidth would be required, and resolution sacrificed. If approximate resonant frequencies are known, the measurements can be carried out with a smaller bandwidth around the estimated resonant frequency. Based on these considerations, a finite-element analysis using ANSYS (version 6.1) was employed to model the first four resonant frequency modes of all the six cantilever beams designed on the test chip [22].

The simulations were performed without a sorbent polymer coating. The cantilever beam is a multilayer structure fabricated from silicon oxide, silicon nitride, polysilicon, and aluminum thin films. In order to perform the modal simulation with ANSYS, the cantilever beam was modeled as a composite
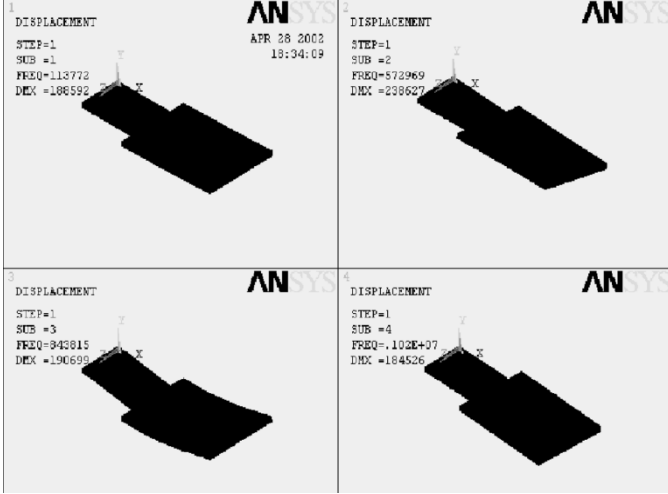
Fig. 5. ANSYS simulation of the cantilever beam 1 resonant frequency. Only the first four modes are represented. The beam dimensions are; beam length 55 μm, beam width 30 μm, plate length 70 μm, width 60 μm, and thickness 4.2 μm.

TABLE I
RESONANT FREQUENCY OF ALL THE BEAMS, SIMULATED
WITH ANSYS AND EXPERIMENTALLY DETECTED

Cantilever #	Simulation results [kHz]	Measured electrically [kHz]
1	113.773	111.550
2	92.380	90.300
3	26.600	25.400
4	29.900	27.350
5	54.100	53.680
6	91.360	89.900

Fig. 6. Interferometer image of the cantilever beam 6. Applied voltage 0 V. The bending of the structure is noted at 7.63 μm.

Fig. 7. Interferometer image of the beam 6. DC 23 V was applied on the interdigitated fingers. The bending of the structure is noted at 7.1 μm.

beam. The mesh elements of all analyzed cantilever beams were made using tetrahedral elements (SOLID 92).

The material properties of the different thin-film composite, such as Young's modulus and density, were taken as previously reported [13]. Squeeze-film damping was not included in the simulation because the beam structures are significantly bent, which reduces effects from air damping.

For cantilever beam 6, the ANSYS simulation of the resonant frequency is shown in Fig. 5, with the four lowest resonant modes. The corresponding cantilever beam SEM image is shown in Fig. 3. The resonant frequencies from the ANSYS simulations of the six cantilever beams fabricated on the chip are provided in Table I.

B. Electrostatic Actuation of the Cantilever Beam

The cantilever beam is excited electrostatically by applying a dc voltage, which results in attractive Coulombic forces between the interdigitated fingers. The cantilever beams are set into oscillatory motion in a plane perpendicular to the beam. This is made possible in part due to the CMU CMOS-MEMS approach, which results in bent structures.

The cantilever beam bending was analyzed with a Wyko NT3300 white light interferometer at CMU. With no applied voltage on the cantilever beam, the bending for cantilever beam 6 is shown in Fig. 6.
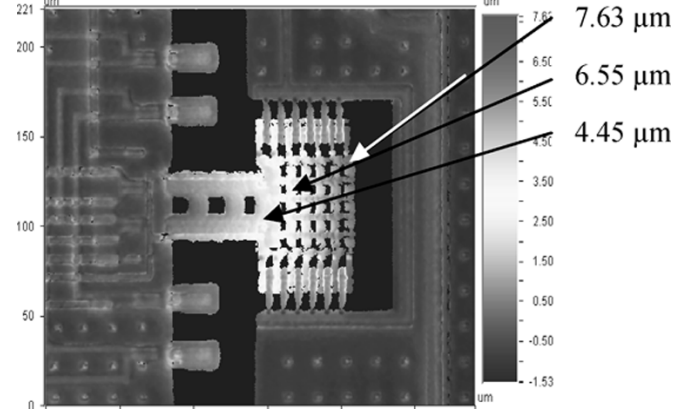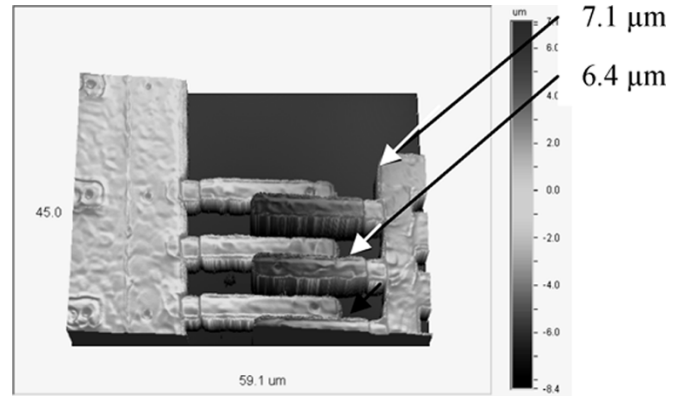
With a dc voltage of 23 V applied to the fingers of cantilever beam 6, the device is shown to deflect toward the support by 0.53 μm, which is large enough for the electrostatic actuation of the cantilever beam. The deflection results are illustrated in the interferometer image shown in Fig. 7.

The dc polarization voltage is applied between the electrodes fingers to create a surface charge and an ac voltage is superimposed to drive the device with a harmonic force. The dc voltage applied from an Agilent E3631A power supply to deflect the cantilever beams was 20 V, and an ac voltage of 4 Vp-p from a Hewlett Packard HP 3588A spectrum analyzer was required to drive the oscillation of the beam.

Two piezoresistors which are part of the Wheatstone bridge are integrated on each beam to monitor the cantilever beam deflections. The output signal from the Wheatstone bridge, which is not amplified, is applied at the input of the spectrum analyzer in order to determine the resonant frequency. At the resonant frequency, the Wheatstone bridge output signal was measured between 80 and 120 mV, depending on the dimensions of each cantilever beam, with the Wheatstone bridge biased at 6 V. The circuitry used to oscillate the cantilever beam is shown in Fig. 8. A simple voltage divider is constructed to superimpose the varying ac voltage on the constant dc voltage.

The resonant frequency simulations with ANSYS were useful to narrow the frequency range monitored by the spectrum analyzer. The resonant frequencies simulated with ANSYS and
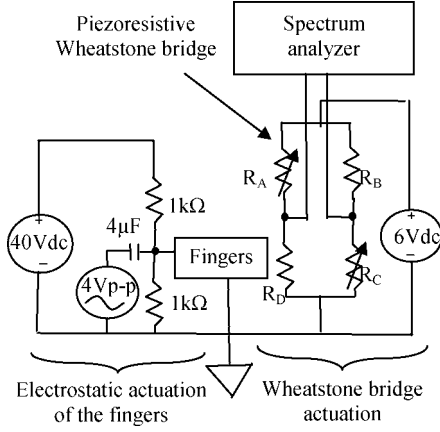
Fig. 8. Schematic of the circuitry used to drive the resonant beam gas sensor.
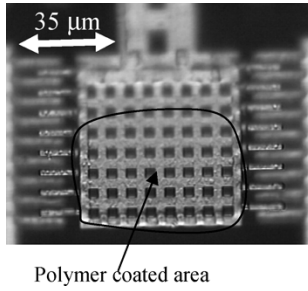

Fig. 9. Polymer drop is deposited close to the beam tip. The device bending results in an image that is out of focus.

measured with the circuitry are in good agreement and are shown in Table I. The differences maybe in part explained by the absence of a complete simulation that would include the fingers and etch release holes.

IV. POLYMER AS ANALYTE SORPTIVE LAYER

The polymer used in this work is a functionalized polycarbosilane, HCSA2. This polymer has been previously described [23], [24] and is a rubbery material with full flowing properties at room temperature. The beam's resonant frequency shift response resulting from analyte sorption increases with increasing thickness of the polymer layer. At equilibrium, the thicker the polymer layer will sorb more gas molecules, with a larger mass change to detect. There are limits to which the device can be practically coated with a polymer film, that relate to the degradation of the cantilever beam quality or Q factor, and slower kinetics with thicker polymer films. The lower Q values are related to an increase in signal noise, which degrades the resolution of the sensor.

The cantilever beam was coated with a dilute solution of polymer HCAS2 in Chloroform (0.03% w/w) with a piezo inkjet dispensing head. The dispensed drop is directed at the desired location on the beam plate by viewing the cantilever beam through a microscope during the coating process. It is important to avoid depositing excessive amounts of polymer on the interdigitated fingers which would prevent oscillation, see Fig. 9. Targeting the drop closer to the cantilever beam tip improves the Q value.
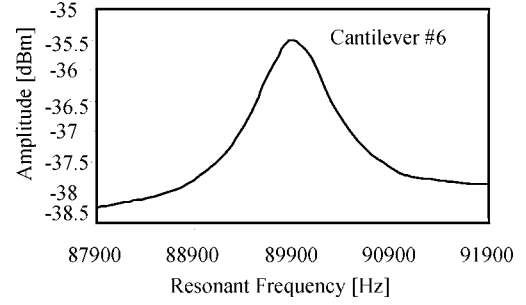

Fig. 10. Resonant frequency of the cantilever beam gas sensor before inkjet coating with polymer was 89.9 kHz.
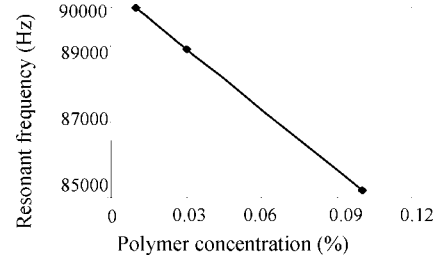

Fig. 11. Change of resonant frequency as a function of the deposited polymer concentration.

Cantilever beam 6 from the chip was coated with a single drop of polymer solution. The resonant frequency of the cantilever beam before coating was 89.9 kHz, as shown in Fig. 10.

The concentrations of polymer used were 0.03% w/w, and 0.1% w/w in chloroform. The inkjet nozzle had an internal diameter of 30 μm; however, the dispensed drop diameter is larger and estimated to be 35 μm. The cantilever beam plate coated with polymer had the dimensions 50×60 μm. To avoid any high-temperature process after polymer coating, the chip was wire bonded onto a Kyocera DIP 40 ceramic package in advance of the polymer coating deposition.

The cantilever beam frequency shift as a function of polymer amount or droplet concentration is shown in Fig. 11, which shows a linear relationship over the range tested. The deposition of the polymer leads to a decrease in resonant frequency, with a simultaneous decrease in the vibrational amplitude and a degradation in the device Q.

V. VAPOR TEST MEASUREMENTS AND RESULTS

The vapor used for cantilever beam testing was generated by bubbling dry N_2 (0.3 – 6 ml/min) through a thermostatted glass container maintained at 15 °C, and diluted from near saturation with a relatively large volume of purified air (100 – 2500 ml/min). The pneumatic tubing used for all gas wetted parts was PFA. The chip mounted in the Kyocera package was sealed by positioning a Combo Lid (Chelsea Technology) over the device package and sealing the peripheral edges by applying tape. The lid had been previously modified by drilling two holes. A single PFA inlet tube (i.d., 0.125") was attached to one of the holes situated directly above the chip, so that airflow was perpendicular to the cantilever beam. The second hole allowed air and vapor to exhaust into the fumehood. The majority of the vapor test measurements were carried out with a constant flow rate (6 ml/min) through the neat DMMP,
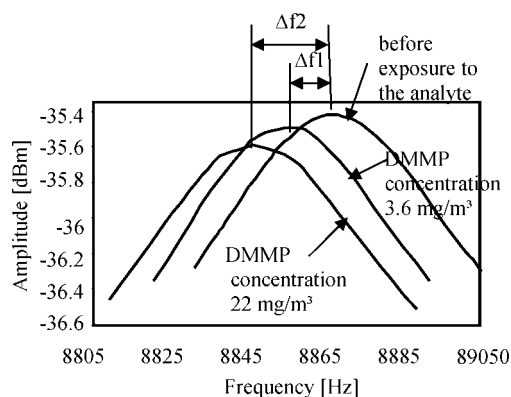
Fig. 12. Cantilever beam response upon exposure to various DMMP concentrations. Frequency shifts are marked $\Delta f1$ and $\Delta f2$.
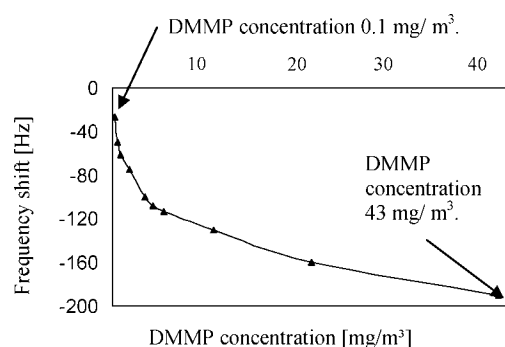

Fig. 13. Cantilever beam response upon exposure to DMMP concentrations varying from 43 to 0.1 mg/ m^3. The detection limit is 0.1 mg/ m^3.

and by carrying the diluent air from 100 to 2500 ml/min. Above 2500 ml/min, the noise of the beam became excessive. The airflow was delivered at a temperature of 20 °C, with a relative humidity (RH) of 0%. The sealed chip manifold was not actively temperature controlled. In a typical experiment, the vapor on and off time periods were fixed at 5 min.

During vapor tests, the cantilever beam was operated as described earlier and the sensor response monitored as a shift in the resonant frequency. The frequency sweep, with a resolution of 5 Hz, over the complete 3-kHz range was set at 5 s. The graphical frequency data, and the resonant frequency were displayed on the spectrum analyzer. The cantilever beam selected for testing was number 6. Initial tests were carried out by exposing a bare cantilever beam to DMMP vapor at elevated concentrations. These experiments showed no measurable frequency shift. The same chip was then coated with a single drop of polymer solution at two different concentrations (0.03% w/w, and 0.1% w/w, in chloroform). This device was then exposed to DMMP vapor at concentrations which were ramped from 43 to 0.1 mg/m^3 in a repeated fashion.

The polymer thickness was estimated from the known solution concentration, the approximate drop volume, and the surface area covered. The computed mean thickness is 335 nm. At this thickness, the sensor time constant to 90% of signal was approximately 10 s. Example frequency sweeps taken from the spectrum analyzer are shown in Fig. 12. The cantilever beam sensor response as a function of DMMP concentration is shown in Figs. 12 and 13. The lowest DMMP concentration tested

was 0.1 mg/m^3 or 20 ppb. At this concentration, the signal frequency shift recorded was 30 Hz, with an estimated signal noise level of 10 Hz.

These measurements were made at 0% RH, but the magnitude of the response to DMMP is not expected to change with increasing humidity, based on tests with the same polymer and a conventional SAW sensor [25]. However, the signal baseline is expected to shift with changing humidity and temperature. Possible solutions to this include signal compensation by actively monitoring the temperature and humidity and using look up tables to adjust the baseline. Alternatively a preconcentrator module can be added up stream of the sensor and if used in an optimum fashion the signal response from water can be isolated from analytes of interest [26].

VI. SUMMARY & CONCLUSION

This device coated with a thin layer of HCSA2 polymer, provides a highly sensitive chemical sensor for the nerve agent class of chemical warfare materials. Measurable signals with DMMP, a stimulant and precursor nerve agent, at the concentration of 0.1 mg/m^3 were observed. The time constant and time recovery for the signal response was of the order of ten seconds to reach ninety percent of equilibrated signal.

In future work, after further device optimization, integrated electronic circuitry will be included with the MEMS structures. In addition, other micromachined analytical system components could be combined together to fabricate a micro gas analyzer. These components may include a micromachined preconcentrator, gas chromatograph, and an air pumping system.

REFERENCES

[1] A. D. McNaught and A. Wilkinson, *IUPAC Compendium of Chemical Terminology*, 2nd ed.   Cambridge, U.K.: Royal Society Chemistry.
[2] J. W. Gardner, V. K. Varadan, and O. O. Awadelkin, *Microsensors, MEMS and Smart Devices*.   New York: Wiley, 2001.
[3] R. A. McGill, M. H. Abraham, and J. W. Grate, "Choosing polymer coatings for chemical sensors," in *Proc. Chemtech*, vol. 24, 1994, pp. 27–37.
[4] D. Diamond, *Principles of Chemical and Biological Sensor*.   New York: Wiley, 1998.
[5] H. Baltes, D. Lange, and A. Koll, "The electronic nose in Lilliput," *IEEE Spectrum*, vol. 35, no. 9, pp. 35–38, Sep. 1998.
[6] H. P. Lang, R. Berger, F. Battiston, J. P. Ramseyer, E. Meyer, C. Andreoli, J. Brugger, P. Vettiger, M. Despont, T. Mezzacasa, L. Scandella, H. J. Guntherodt, C. Gerber, and J. K. Gimzewski, "A chemical sensor based on micromechanical cantilever array for the identification of gases and vapors," *Appl. Phys. A*, vol. 66, pp. S61–S64, 1998.
[7] T. A. Betts, C. A. Tipple, M. J. Sepaniack, and P. G. Datskos, "Selectivity of chemical sensors based on micro-cantilevers coated with thin polymer films," *Anal. Chim. Acta.*, vol. 422, pp. 89–99, 2000.

[8] G. Muralidharan, A. Wig, L. A. Pinnaduwage, D. Hedden, T. Thundat, and R. T. Lareau, "Adsorption-desorption characteristics of explosive vapors investigated with microcantilevers," *Ultramicroscopy*, vol. 97, pp. 433–439, 2003.

[9] A. Hierlemann, O. Brand, C. Hagleitner, and H. Baltes, "Microfabrication techniques for chemical/biosensors," *Proc. IEEE*, vol. 91, no. 6, pp. 839–863, Jun. 2003.

[10] F. M. Battiston, J. P. Ramseyer, H. P. Lang, M. K. Baller, C. Gerber, J. K. Gimzewski, E. Meyer, and H. J. Guntherodt, "A chemical sensor based on microfabricated cantilever array with simultaneous resonant-frequency and bending readout," *Sens. Actuators B*, vol. 3849, pp. 1–10, 2001.

[11] W. T. Thomson, *Theory of Vibration with Applications*, 4th ed. Upper Saddle River, NJ: Prentice-Hall, 1993.

[12] J. Zhou, P. Li, S. Zhang, Y. Long, F. Zhou, Y. Huang, P. Yang, and M. Bao, "Zeolite-modified microcantilever gas sensor for indoor air quality control," *Sens. Actuators B*, vol. 94, pp. 337–342, 2003.

[13] D. Lange, O. Brand, and H. Baltes, *CMOS Cantilever Sensor System*. New York: Springer, 2002.

[14] D. Lange, C. Hagleitner, O. Brand, and H. Baltes, "CMOS resonant beam gas sensing system with on-chip self excitation," in *Proc. IEEE 14th Int. Conf. MEMS*, Jan. 2001, pp. 547–552.

[15] I. Voiculescu, M. Zaghloul, R. A. McGill, E. Houser, J. Vignola, and D. Jones, "Modeling and measurements of a composite microcantilever beam with applications for chemical gas sensors," *J. Micromech. Microeng.*, to be published.

[16] T. Thundat, E. A. Wachter, S. L. Sharp, and R. J. Warmack, "Detection of mercury vapor using resonating microcantilevers," *Appl. Phys. Lett.*, vol. 66, no. 13, pp. 1695–1697, 1995.

[17] H. Xie, L. Erdmann, X. Zhu, K. J. Gabriel, and G. K. Fedder, "Post-CMOS processing for high-aspect-ratio integrated silicon microstructures," *J. Microelectromech. Syst.*, vol. 11, pp. 93–101, 2002.

[18] G. K. Fedder, S. Santhanam, M. L. Reed, S. C. Eagle, D. F. Guillou, M. S. -C. Lu, and L. R. Carley, "Laminated high-aspect-ratio microstructures in a conventional CMOS process," *Sens. Actuators A*, vol. 57, pp. 103–110, 1996.

[19] D. F. Guillou, S. Santhanam, and L. R. Carley, "Laminated, sacrificial-poly MEMS technology in standard CMOS," *Sens. Actuators A*, vol. 85, pp. 346–355, 2000.

[20] [Online]. Available: www.ece.cmu.edu/research/chips/openhouse0501/Gary.pdf

[21] C. Vancura, M. Ruegg, Y. Li, D. Lange, C. Hagleitner, O. Brand, A. Hierlemann, and H. Baltes, "Magnetically actuated CMOS resonant cantilever gas sensor for volatile organic compounds," in *Proc. 12th Int. Conf. Solid State Sensors, Actuators and Microsystems, Transducers*, vol. 2, Boston, MA, Jun. 2003, pp. 1355–1358.

[22] O. Brand, H. Baltes, and U. Baldenweg, "Thermally excited silicon oxide beam and bridge resonators in CMOS technology," *IEEE Trans. Electron Devices*, vol. 40, no. 10, pp. 1745–1753, Oct. 1993.

[23] E. J. Houser, D. L. Simonson, J. L. Stepnowski, and R. A. McGill, "Linear and hyperbranched hydrogen bond acidic poly(silylene methylene)s for chemical sensor applications," *PMSE Preprints*, vol. 88, p. 548, 2003.

[24] R. A. McGill and E. J. Houser, "Linear Chemoselective carbosilane polymers and methods for use in analytical and purification applications," U.S. Patent 6 660 230.

[25] A. McGill, private communication.

[26] R. A. McGill, V. K. Nguyen, R. Chung, R. E. Shaffer, D. DiLella, J. L. Stepnowski, T. E. Mlsna, D. L. Venezky, and D. Dominguez, "The NRL-SAWRHINO: A nose for toxic gases," *Sens. Actuators B*, vol. 65, no. 1, pp. 10–13, Jun. 2000.

Ioana Voiculescu received the Ph.D. degree in mechanical engineering from Politehnica University, Timisoara, Romania, in 1997, and the Ph.D. degree in mechanical engineering (with an emphasis in MEMS) from The George Washington University, Washington, DC, in 2005.

She was an Assistant Professor for ten years at Politehnica University. She is currently a Research Associate at the Naval Research Laboratory, Washington, DC. Her research interests are in the area of MEMS design, fabrication, and testing.

Mona E. Zaghloul (F'80) received the M.A.Sc. degree in electrical engineering in 1970, the M.Math. degee in computer science and applied analysis in 1971, and the Ph.D. degree in electrical engineering from the University of Waterloo, Waterloo, ON, Canada in 1975.

She is currently a Professor in the Electrical and Computer Engineering Department, The George Washington University, Washington, DC, where she was the Chair of the department from 1994 to 1998, and where she also directs the Institute of MEMS and VLSI Technology. The Institute of MEMS and VLSI Technology encompasses several interdisciplinary faculties and over a dozen graduate students with funding from several agencies. She has worked extensively in the general areas of circuits and systems, nonlinear systems, and microelectronic systems since 1975. She has published over 200 technical papers and reports in the areas of circuits and systems theory, nonlinear system theory, micromachining MEMS sensors design, and micro-electronic VLSI analog and digital circuits design, and has contributed to four books. Since 1984, she has been with the National Institute of Standards and Technology (NIST), Semiconductor Devices Technology Division, Gaithersburg, MD.

Dr. Zaghloul received the 50th year Gold Jubilee Medal from the IEEE Circuits and Systems Society in recognition for outstanding contribution to the society. She is currently an Associate Editor for the IEEE SENSORS JOURNAL. She was the Vice President of IEEE-CAS Technical Activities (1999 to 2001).

R. Andrew McGill received the B.Sc. degree (with honors) and the Ph.D. degree in chemistry from the University of Surrey, Surrey, U.K., in 1984 and 1988, respectively, followed by a two-year postdoctoral position.

He is the Head of the Materials and Sensors Section, U.S. Naval Research Laboratory (NRL), Washington, DC. He has been with the NRL since 1991, and as a member of the NRL technical staff since 1995. In 1998, he formed the Materials and Sensors Section. His research interests span basic and applied areas, including molecular interactions, rational materials design, synthesis of functionalized sorbent materials/polymers, MEMS and micromachined-based devices, and chemical, biological, and explosives sensors/detectors for monitoring toxic and hazardous materials.

Eric J. Houser received the Ph.D. degree in inorganic chemistry from the University of Illinois, Urbana, IL, in 1995.

He is currently a Research Chemist at the Naval Research Laboratory, Washington, DC, in the Materials and Sensors branch of the Materials Science and Technology Division. His research interests include chemical sensing, MEMS, carbon nanotube materials and devices, high-temperature materials, molecular electronics, transition metal cluster catalysis, and metal-metal bond reactivity.

Gary K. Fedder received the B.S. and M.S. degrees in electrical engineering from the Massachusetts Institute of Technology in 1982 and 1984, respectively, and the Ph.D. degree from the University of California, Berkeley, where his research resulted in the first demonstration of multimode control of a underdamped surface-micromachined inertial device. .

He is a Professor at Carnegie Mellon University, Pittsburgh, PA, holding a joint appointment with the Department of Electrical and Computer Engineering and The Robotics Institute. From 1984 to 1989, he was with the Hewlett-Packard Company, where he worked on on circuit design and printed-circuit modeling. Currently, he serves on the editorial board of the IOP *Journal of Micromechanics and Microengineering* and as Co-Editor of the Wiley-VCH *Sensors Update* and *Advanced Micro- and Nanosystems* book series. He has contributed to over 100 research publications and several patents in the MEMS area. His research interests include microsensor and microactuator design and modeling, integrated MEMS manufactured in CMOS processes, and structured design methodologies for MEMS.

Dr. Fedder received the 1993 AIME Electronic Materials Society Ross Tucker Award, the 1996 Carnegie Institute of Technology G. T. Ladd Award, and the 1996 NSF CAREER Award. Currently, he serves as a subject editor for the IEEE/ASME JOURNAL OF MICROELECTROMECHANICAL SYSTEMS.